ORIGINAL PAPER

Fabrication, Characterisation and Tribological Investigation of Artificial Skin Surface Lipid Films

**L.-C. Gerhardt · A. Schiller · B. Müller ·
N. D. Spencer · S. Derler**

Abstract This article deals with the tribology of lipid coatings that resemble those found on human skin. In order to simulate the lipidic surface chemistry of human skin, an artificial sebum formulation that closely resembles human sebum was spray-coated onto mechanical skin models in physiologically relevant concentrations (5–100 µg/cm^2). Water contact angles and surface free energies (SFEs) showed that model surfaces with $\leq$25 µg/cm^2 lipids appropriately mimic the physico-chemical properties of dry, sebum-poor skin regions. In friction experiments with a steel ball, lipid-coated model surfaces demonstrated lubrication effects over a wide range of sliding velocities and normal loads. In friction measurements on model surfaces as a function of lipid-film thickness, a clear minimum in the friction coefficient (COF) was observed in the case of hydrophilic, high-SFE materials (steel, glass), with the lowest COF ($\approx$0.5) against skin model surfaces being found at 25 µg/cm^2 lipids. For hydrophobic, low-SFE polymers, the COF was considerably lower (0.4 for PP, 0.16 for PTFE) and relatively independent of the lipid amount, indicating that both the mechanical and surface-chemical properties of the sliders strongly influence the friction behaviour of the skin-model surfaces. Lipid-coated skin models might be a valuable tool not only for tribologists but also for cosmetic chemists, in that they allow the objective study of friction, adhesion and wetting behaviour of liquids and emulsions on simulated skin-surface conditions.

1 Introduction

Human skin is our "living envelope" and the largest organ, covering a surface area of between 1.6 and 2 m^2 in adults [1]. The surface is usually protected by an acidic hydro-lipid film (pH 4–6), which controls skin flora, prevents colonisation of the skin by pathogenic species, and acts as defence against invading microorganisms [1]. The hydro-lipid film is composed of water and sebum, which are excreted from sweat and sebaceous glands, respectively. Water and sebum move towards the skin surface and cover the *stratum corneum* (SC) as a water–oil emulsion. The SC can be described in terms of a brick-and-mortar model [2], in which the corneocytes (bricks) are embedded in lamellar epidermal lipids (mortar) [3], which function as an efficient barrier against extreme water loss.

In the past, several chemical SC models were developed and characterised regarding lipid phase behaviour [4–6], lamellar organisation/orientation [7], kinetics of barrier formation [8] and permeation properties [9, 10]. Using silicone replicas from skin, Charkoudian prepared a

L.-C. Gerhardt · A. Schiller · S. Derler (✉)
Laboratory for Protection and Physiology, Empa, Swiss Federal Laboratories for Materials Testing and Research, Lerchenfeldstrasse 5, CH-9014 St. Gallen, Switzerland
e-mail: Siegfried.Derler@empa.ch

L.-C. Gerhardt · N. D. Spencer
Laboratory for Surface Science and Technology, Department of Materials, ETH Zurich, Zurich, Switzerland

B. Müller
Laboratory for Advanced Fibres, Empa, Swiss Federal Laboratories for Materials Testing and Research, St. Gallen, Switzerland

micro-structured gelatine-based lipid model surface for testing and assessing adhesion of medical tapes to the skin [11].

There is, however, an increasing scientific interest in the tribological properties of lipids [12], as well as in the development of mechanical skin models. Skin models are of general importance in the objective, reliable and time-saving assessment of skin friction against external contact materials (e.g. when touching/handling objects, wearing clothes, or shaving the skin). In this connection, lipid-coated skin models and an artificial sebum formulation, respectively, could be used for studying not only the frictional and optical properties of skin or hairs, but also the release and absorption of chemicals from materials in contact with skin. In particular, soft elastomers (e.g. silicones) have been investigated as candidate materials in studies focussing on viscoelastic, mechanical skin models [13, 14]. We have recently shown that a polyurethane-coated polyamide fleece with a surface topography and roughness close to that of human skin is an appropriate mechanical skin equivalent for the objective assessment of fabric friction [15]. However, this model does not take into account the surface chemistry of human skin.

So far, the application of an artificial sebum formulation to skin models has not been reported in the literature, and the simulation of skin lubrication remains largely unexplored. Coatings with sebum-like lipids might therefore be a promising path for mimicking the surface lipid chemistry of the SC, which is considered to play an important role in skin tribology [16–19]. Sivamani et al. [19] reviewed the current state of skin tribology. It is generally acknowledged that skin-friction depends on the type of contacting materials, as well as on the physiological skin condition (e.g. hydration state [15, 20, 21]) and on mechanical contact parameters, especially on the normal load and the sliding velocity [20, 22–24] as a consequence of the viscoelastic material properties of human skin. The role of sebum lipids and their interactions with water have not been fully elucidated yet [16, 17, 25, 26] and were controversially

debated. Gupta et al. [16] found a positive relationship between sebum level and forearm skin-friction, whereas Cua et al. [17] observed practically no correlation between both parameters for eleven different skin sites and suggested that surface lipids might play a limited role for skin-friction.

In this article, we report on the fabrication and characterisation of improved, lipid-coated skin models for the simulation of skin lubrication. Skin-relevant lipid mixtures were applied to an existing skin-simulating material in order to mimic the lipidic components of the hydro-lipid film of dry skin. The objectives were (a) to produce a realistic artificial sebum formulation, (b) to prepare lipid films with physiologically relevant concentrations (5–100 µg/cm^2), and (c) to characterise the physico-chemical properties (hydrophobicity, surface energy), as well as the tribological behaviour of lipid-coated skin models against different spherical sliders.

2 Materials and Methods

2.1 Artificial Sebum

A synthetic sebum formulation, which reflects the correct lipid class composition of human sebum and its relative proportions of saturated and unsaturated acyl chains, has been adopted from the literature [27, 28]. Native sebum contains $\approx 32\%$ triglycerides, $\approx 25\%$ wax esters, $\approx 27\%$ free fatty acids, $\approx 6\%$ sterols, and $\approx 10\%$ squalene [1]. On this basis, an artificial sebum formulation (Table 1) consisting of nine lipids in proportions that closely resemble human sebum has been produced [28]. A stock solution (10 g/L) with a total mass of 5 g of lipids was prepared at room temperature by dissolving appropriate amounts of all the listed chemicals in 0.5 L of chloroform-methanol solvent (2:1). The stock solution was magnetically stirred for ≈ 15 min at 23 °C and 50% relative humidity to ensure complete dissolution and mixing of the lipids, and was

Table 1 Composition of the artificial sebum formulation

Lipid class	Saturation	Chemical	Amount (%)	Molarity (mM)
Triglycyerides	Saturated	Tristearin	21.4	1.20
	Unsaturated	Triolein	10.7	0.60
Wax esters	Saturated	Palmityl palmitate	19.4	2.02
	Unsaturated	Oleyl oleate	4.8	0.46
Free fatty acids	Saturated	Stearic acid	13.8	2.42
	Unsaturated	Oleic acid	13.8	2.43
Cholesterol ester		Cholesteryl oleate	1.9	0.15
Free cholesterol		Cholesterol	3.9	0.50
Squalene		Squalene	10.3	1.25

further diluted to concentrations of 5, 2.5, 1, 0.5 g/L. All chemicals were purchased from Sigma-Aldrich (Schnell-dorf, Germany). Tristearin and cholesteryl oleate were of technical grade, triolein of practical grade ($\approx 65\%$). All other lipids had purities of $\geq 95\%$, and the solvents were of analytical grade.

2.2 Skin Model Substrate and Film Preparation

A polyurethane-coated polyamide microfibre fleece (Lorica soft®, Lorica Sud, Milan, Italy) showing a surface topography and roughness similar to that of human skin (Table 2) was chosen as a model substrate [15, 22, 29, 30]. Pump vapouriser bottles (Type 215-6274, VWR, Dietikon, Switzerland) were used to manually spray the lipid mixtures onto the substrates, as described in detail in [31]. The volume of five pump cycles (5×100 μL) was applied to an area of 50 cm^2 (size: 12.5 cm $\times$ 4 cm) from a distance of approximately 5 cm. The films were then carefully covered with plastic caps (internal height ≈ 1 cm) for about 1 h to ensure slow solvent evaporation, allowing effective spreading and adsorption of the lipids on the model skin surface.

The as-prepared films had theoretical average concentrations of 5, 10, 25, 50 and 100 μg/cm^2, which represent a range of sebum concentrations on different anatomical sites [1, 32]. Lipid concentrations were calculated on the basis of the dissolved lipid amounts and the sprayed volume, assuming a homogeneous distribution of the lipids on the substrate. Using these results, lipid film thicknesses were determined considering a sebum density of 0.91 g/cm^3 [1].

The nominal thickness of the films was in the range 0.11–1.1 μm, which is in the order of skin surface lipid film thicknesses in vivo [32], and about 20–200 times greater than the thickness of a lipid bilayer [33]. A solely solvent-treated substrate served as a control. All lipid films were freshly prepared on the evening before tribological testing and other experimental analyses, in order to avoid alterations of the lipids or possible influences due to ageing/

oxidation of the unsaturated lipids [28]. All lipid coatings were preconditioned for at least 12 h under controlled laboratory conditions (20 ± 1 °C, $65 \pm 5\%$ relative humidity). All the films were prepared by the author (L.-C.G) to standardise the fabrication method.

2.3 Lipid Film Characterisation

2.3.1 Iodine Staining Method

The homogeneity of the dispersion of the lipids was assessed by the iodine-vapour-staining method. Exposed to iodine vapour, an electrophilic addition of iodine to the carbon–carbon double bond of unsaturated lipid chains takes place (Fig. 1).

Since the solely solvent-treated skin model Lorica became stained by the iodine vapour, a chromatography filter paper (saturation pad, Type 22.5243, CAMAG, Muttenz, Switzerland) was alternatively employed as substrate to visualise the dispersed lipids. Iodine crystals (≈ 3 g) were placed in a round glass chamber (volume: 0.5 L) and allowed to sublimate at room temperature until the jar was saturated with iodine vapour. Subsequently, the filter paper specimens with and without lipids were vertically placed into the jar and exposed to the iodine vapour for 3 min. Due to the reaction shown in Fig. 1, the initially unstained, lipid-coated filter papers fabricated in the same way as described in Sect. 2.2, turn to a deeply yellow or brown colour depending on the concentration of lipids applied (Fig. 2).

### 2.3.2 Scanning Electron Microscopy (SEM)

All skin models were inspected with a field-emission scanning electron microscope (FEG-SEM S-4800, Hitachi, Tokyo, Japan) using a secondary-electron detector operating in a high-vacuum mode (<1 mPa) and 15-kV accelerating voltage. Surface morphology, film homogeneity and changes in the microstructure upon the friction process were qualitatively assessed. The samples were sufficiently conductive so that no special sample preparation or sputtering was necessary.

Table 2 Surface roughness values of the artificial leather Lorica compared with those for different skin sites of persons aged between 20 and 40 years

Surface	R_a (μm) (range)	R_z (μm) (range)
Lorica original [15]	14.9 ± 1.7 (11–18)	91.3 ± 10.5 (76–103)
Index finger [22]	26.1 ± 6.1 (19–33)	87.3 ± 17.1 (62–99)
Edge of hand [22]	14.9 ± 6.7 (9–22)	54.1 ± 21.2 (33–73)
Back of hand [30]	(23–28)	(138–144)
Volar forearm [30]	(17–20)	(119–125)
Volar forearm [29]	(12–13)	(82–92)
Forehead (temple) [29]	(12–15)	(84–95)
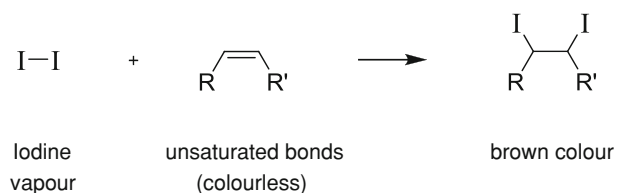
Fig. 1 Simplified reaction scheme: electrophilic addition of iodine to a double bond of a lipid
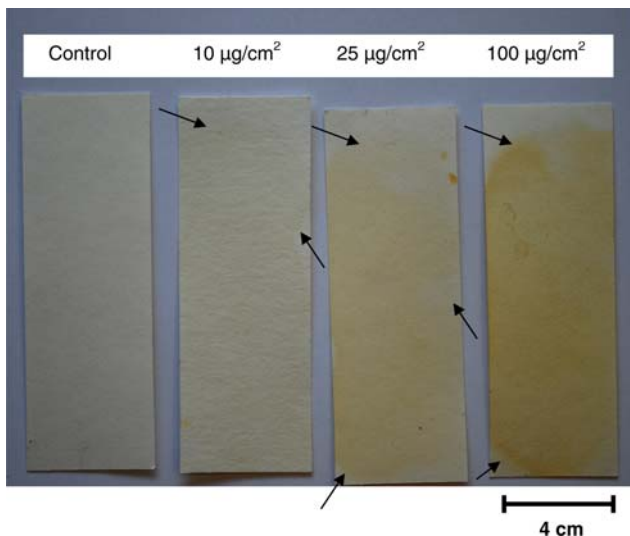
Fig. 2 Photographs of fabricated lipid coatings showing a homogeneous as well as an increasing yellow stain with lipid content upon exposure to iodine vapour, which indicates well-distributed lipids on the filter paper. Arrows refer to fringes surrounding the circular stains (stain circles), as well as imperfections due to the manual spraying process

2.3.3 Contact Angle Measurements

The chemical properties of skin-model surfaces were assessed with a DSA-100 (KRÜSS, Hamburg, Germany) contact angle (CA) measurement instrument, operating at (22 ± 1) °C and (50 ± 5)% relative humidity. A drop of 4–5 μL was gently deposited onto the respective surface, and static CAs recorded within 10 s after deposition to minimise evaporation of volatile fluids and measurement uncertainty due to time-dependent spreading of the liquid over the rough skin model surfaces. Contact angles were calculated using a circular algorithm method, implemented in the KRÜSS Drope Shape Analysis software (DSA 3, Release 1.60).

Hydrophobicity/hydrophilicity of the surfaces was determined by assessment of water CAs. The surface free energy (SFE) of the skin model surfaces was determined according to the method proposed by Owens, Wendt, Rabel and Kaelble [34–36], as described in detail in [37]. Measurements were performed using three liquids with different polar and dispersive components, ultrapure water (resistivity: 18.2 MΩ/cm), ethylene glycol, and hexadecane (both analytical grade, Fluka, Schnelldorf, Germany). At least 15 CAs were measured per liquid, on three different locations of at least five separate models, with and without lipids.

The physico-chemical surface properties of the different slider materials (Sect. 2.4) were investigated using the same methods and a CA measurement system G10 (KRÜSS, Hamburg, Germany).

2.4 Friction Experiments

Sliding friction experiments were carried out using the textile friction analyser, as described elsewhere [38]. Briefly, spheres of various solids (polished stainless steel X5 CrNi 18–10, smooth glass, PP, PTFE, Ø 10 mm) were rubbed in a reciprocating motion against the different skin models (thickness of Lorica: 1.1 mm). Every 50 cycles, the mean dynamic sliding friction coefficient (COF) was calculated from the ratio of friction force to normal force. Friction measurements were performed over at least 50 cycles allowing friction to be studied following possible running-in effects. In the friction experiments, the influence of lipid concentration, normal load and sliding velocity on the COF against diverse materials was investigated as a function of rubbing cycles. New samples of skin models were used for each test, and the solid spheres were cleaned with 70% ethanol before each experiment. At least four tests were carried out per skin model. Data are presented as mean $\pm$ 1 standard deviation (SD).

3 Results and Discussion

3.1 Film Characterisation

Iodine staining as well as SEM revealed a homogeneous lipid distribution. There was a notable increase in the yellow stain for the lipid-coated filter papers compared to the solvent-treated control filter paper, with the deepest yellowish colour appearing for the 100 μg/cm^2 lipid coating (Fig. 2). SEM images indicated that an increasing amount of lipids present on the skin-model substrate resulted in rougher surfaces (Fig. 3).

Water CAs ranged from $(74.4 \pm 3.6)°$ for the solvent-treated control skin model (SMC) to $(120.7 \pm 3.9)°$ for the model surface with 100 μg/cm^2 lipids (SM100) (Table 3). Treatment by the solvents rendered the originally hydrophobic, almost non-polar artificial leather (Water CA $\approx 110°$) to be hydrophilic and highly polar. This alteration in the surface chemistry probably arises from the removal of substantial amounts of dibutylphthalate plasticiser, as shown by GC–MS analysis (HP 5890 GC, HP 5989A MS-ENGINE, Hewlett-Packard, Avondale, USA).

The range of water CAs (74–121°), as well as the gradual increase in the water CA with increasing lipid amount suggest that the upper lipid layer is randomly oriented rather than well organised. It has been reported that supported lipid bilayers are unstable upon exposure to air since the lipids spontaneously rearrange themselves [39]. With increasing amount of lipids, the model surfaces became more hydrophobic and non-polar, concurrent with a tendency to lower SFE. The dispersive (non-polar)

Fig. 3 SEM micrographs of the as-fabricated, unrubbed skin model surfaces: **a** the solvent-treated control skin model exhibits a relatively smooth surface topography with bumps and bulges (**a2**). **b** The coating with 10 μg/cm² lipids appears rougher compared to the control and shows relatively homogeneous lipid dispersion. The bumps are partially covered with lipids (arrows, **b2**). **c** The coating with 100 μg/cm² lipids shows a distinctive rough surface structure that seems to be substantially covered by lipids. Typical lipid "flakes" can be observed at higher magnifications (**c2**)

1 mm   50 μm
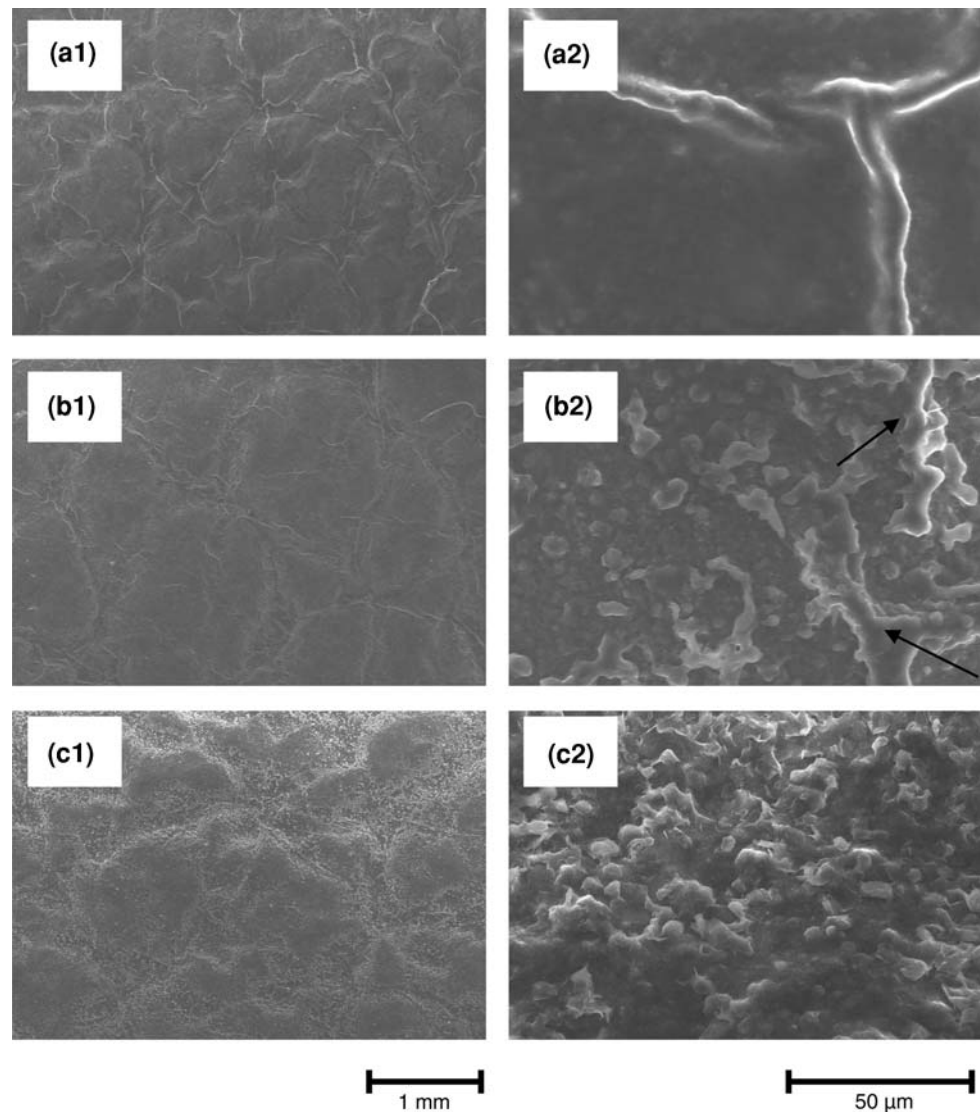
Table 3 Water contact angles of the different skin model surfaces, as well as SFE (γ_S) separated into the dispersive (γ_S^D) and polar (γ_S^P) fraction

Model surface	Water CA (°)	γ_S (mN/m)	γ_S^D (mN/m)	γ_S^P (mN/m)
Lorica original	110.0 ± 1.7	19.7	19.6	0.1
Solvent-treated control	74.4 ± 3.6	33.4	23.6	9.8
5 μg/cm² lipids	75.0 ± 4.4	32.9	23.2	9.8
10 μg/cm² lipids	79.9 ± 4.3	29.9	22.1	7.8
25 μg/cm² lipids	93.5 ± 2.7	25.0	22.3	2.7
50 μg/cm² lipids	105.9 ± 3.2	21.3	21.0	0.3
100 μg/cm² lipids	120.7 ± 3.9	24.6	24.1	0.5

component of the SFE, however, remained quite constant (Table 3).

Extracted human sebum has a viscosity of 171 mPa·s at 20 °C [40]. However, the physiological viscosity of human sebum is probably lower because of superficial water (usually from sweat), with which the lipids can interact to form a water–sebum emulsion on the skin surface.

The fabricated lipid coatings corresponded to physiological concentrations usually found on human skin [1, 32]. Lipid film thickness of less than 0.5 μm was observed on sebum-poor skin areas (forearm, extremities) and greater than 4 μm in areas of the sebum-rich facial skin [32]. On the former skin areas, lipid amounts of ≤10 μg/cm² are usually found, whereas on the latter

sites sebum concentrations can exceed 100 µg/cm^2 [1, 32].

The SFEs and water CAs we found for the different model surfaces are in a good agreement with values reported in the literature for human skin in vivo. Elkhyat et al. [18] measured a static water CA of 91.2° on the volar forearm and 97° on the sebum-poor abdomen, which is close to the model surface with 25 µg/cm^2 lipids. Elkhyat et al. further reported a SFE of 38.5 mN/m on the volar forearm, with a dispersive fraction of 27.6 mN/m [41], which places the forearm among almost non-polar, low-energy surfaces.

However, the trend to higher hydrophobicity and lower SFE for skin models with increasing lipid content was in contrast to in vivo data published for different anatomical sites with varying amounts of sebum [26]. Mavon et al. reported water CAs of 88° on the sebum-poor forearm and of 55° on the sebum-rich forehead [26]. They further showed that sebum lipids increase human skin SFE, being (38.7 ± 6.4) mN/m on the forearm and (42.5 ± 3.9) mN/m on the lipid-rich forehead [26]. The dispersive components remained fairly constant, confirming the results of this study (Table 3).

Mavon et al. suggested that sebum gives the skin surface a hydrophilic character, but questioned the mechanisms behind the wetting-enhancing effect of sebum [26]. In particular, free fatty acids (abundant on sebum-rich skin surfaces) might play an important role for the wetting-enhancing effect of sebum and seem to interact with the compounds of the sebum-sweat emulsion in such a way that they change the physico-chemical properties of the skin surface [25, 26]. Owing to its amphiphilic character, sebum has the ability to convert hydrophobic surfaces to slightly hydrophilic, and vice versa, if they interact with the surface through a specific functional group.

The discrepancy in the SFE and water CA data between in vivo results and this study might also be due to greater sweat-gland density and higher skin moisture content on the sebum-rich forehead in comparison to volar forearm skin [1].

3.2 Friction Experiments: Influence of Lipid Concentration

The durability and long-term behaviour of the lipid films were observed over a period of 400 friction cycles using a steel ball as tribo-partner (Fig. 4). All lipid skin model surfaces showed lubrication effects and lower friction than the solvent-treated SMC throughout the experiments, indicating the stability of the coatings. Initial COFs ranged from 0.43 for the skin model with 25 µg/cm^2 lipids (SM25) to 0.61 (SMC). Final COFs varied between 0.62 for the model with 100 µg/cm^2 lipids (SM100) and 0.94 (SMC).
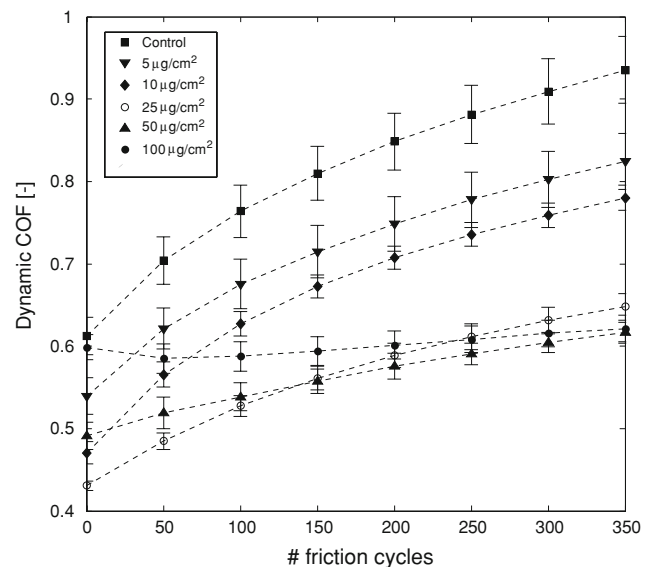
Fig. 4 Time-dependence of the dynamic COF for a steel ball against different skin model surfaces. Different friction patterns were found. Tests ($n = 5$) were carried out with a normal load of 2 N and a mean sliding speed of 62 mm/s. Note that the curves are shifted to the left by 50 friction cycles

In tribo-systems, depending on the presence and amount of lubricants, as well as the minimum separation in the lubricant film between the contacting surfaces, the friction force can be produced by four different physical mechanisms: (a) dry friction, (b) boundary friction, (c) mixed friction and (d) hydrodynamic friction. In cases where the lubricant film does not completely separate the surfaces, the friction results from the contact of lubricated surface asperities and from shearing of the thin lubricant film that adheres to the tribo-counterfaces [42].

Due to the small nominal lipid film thickness (≤ 1.1 µm) and the high roughness value ($R_z = 91$ µm) of the polymer skin model substrate (Table 2), we consider the system under the given test conditions (normal load: 2 N, sliding velocity: 62 mm/s or ≤ 100 mm/s in Sect. 3.3) in the boundary lubrication regime (for uncoated skin models: dry friction).

Under boundary lubrication conditions, the friction of a spherical rigid indenter against a compliant polymer surface is characterised by contributions from adhesion and deformation in the form of hysteresis and ploughing [42, 43]. The thin sebum lipid layer can be considered as a viscous lubricant film, so that the adhesion component of friction—arising from surface forces between the lubricated asperities of the skin model and the steel sphere—is greatly affected by the amount of lipids. Consequently, in boundary-lubricated systems, the overall COF can be written as [42]:
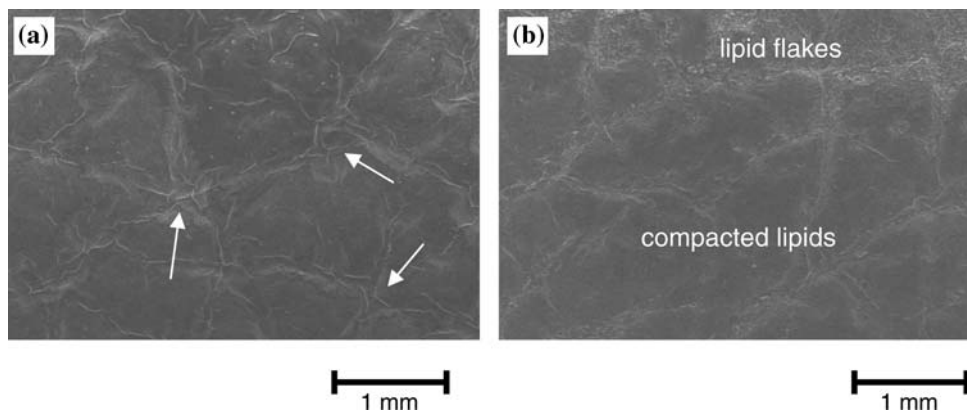
$$\mu = \mu_{\text{adhesion}} + \mu_{\text{hysteresis}} + \mu_{\text{ploughing}} \tag{1}$$

In general, the tendency to lower friction for lubricated surfaces can be attributed to both the suppression of

adhesive van der Waals forces and the reduction of the shear strength of the lubricated contact points [42, 44]. Increase of friction can be ascribed to greater adhesive/attractive forces (e.g. capillary forces) and greater real contact area (RCA). Thus, in the friction contact of the steel ball against the different lipid films, the combination of two competitive effects, namely, interfacial shear strength (ISS) and RCA, influences the adhesion component of friction and can be used to qualitatively interpret the experimental data.

On the basis of SEM images (Fig. 5) and friction curves obtained from repetitive experiments on the same skin model, the strongly increasing COFs for the SMC (Fig. 4), as well as for skin models with 5 and 10 $\mu g/cm^2$ lipids (SM5, SM10), can be reasonably explained by viscoplastic asperity flattening and irreversible deformation that increase the RCA. These effects are assumed to be more important than shear strength reduction provided by the lipid layer on the model substrate. With increasing lipid amount, the surface of the skin-model substrate seems to become protected from the former effects, leading to lower rises in the COF with rubbing time.

The relatively high initial COF of 0.60 for SM100 (Fig. 4) indicates substantial adherence of lipids to the steel ball leading to greater RCA due to the high amount of lipids on the surface. In addition, the relatively stable friction trace for SM100 suggests that viscoplastic asperity flattening and depletion of lipids (Fig. 5) were less pronounced than for SM10, and that a relatively constant RCA and adhesion component may dominate the friction behaviour. In all the skin models investigated, capillary bridges from moisture condensation are unlikely due to the hydrophobic nature of the skin model surfaces (water CAs: 74–121°, Table 3).

3.3 Friction Experiments: Influence of Sliding Velocity

Two contrasting cases, SM10 and SM100, were further investigated and compared with the tribological behaviour of the SMC. The influence of sliding velocity on the COF is shown in Fig. 6.

Both lipid-coated skin model surfaces showed lubrication effects over the range of sliding velocities investigated (8.4–100 mm/s). Only at low speeds (<20 mm/s), did the COF measured against SM100 exceed that of SMC, indicating increased adhesion and contact area, probably provided by compressed lipid flakes (see Figs. 3c2 and 5b). High lipid loadings on the skin-model substrates could lead to sticking effects, explaining the systematically higher COFs of the steel ball measured against SM100 in comparison to SM10 (Fig. 6).

Several factors can contribute to the increase in the COF with sliding velocity. First, thermal effects could increase adhesion at high sliding speeds. Due to the low heat

Fig. 6 Influence of sliding velocity on the dynamic COF after 100 friction cycles. Tests ($n = 5$) were carried out with a normal load of 2 N
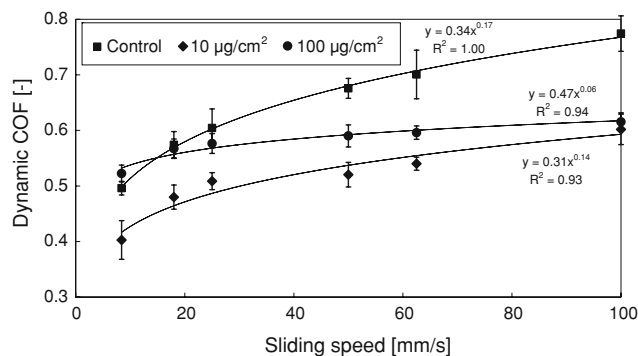
Fig. 5 SEM micrographs after 400 friction cycles at a normal load of 2 N: **a** Plastic deformation (asperity flattening) of the solvent-treated skin model surface can be observed (arrows). The bulges/elevations of the surfaces appear flattened compared to the unrubbed skin model (see Fig. 3a1). **b** Compared to the unrubbed state (see Fig. 3c1), no

clear asperity flattening or plastic deformation can be observed for the skin model surface with 100 $\mu g/cm^2$ lipids after the friction process. Areas with loose lipid flakes can be distinguished from zones, in which the lipids seem to be compacted, filling in the interspaces between the bulges

conductivity, local heating-up of a polymer as a consequence of frictional heat is usually associated with material softening and increase in RCA, adhesion and friction [45, 46]. Thermal effects are most distinctive for the uncoated skin model, leading to the strongest rise in COFs with values ranging from ≈ 0.5 to ≈ 0.75 (Fig. 6). In contrast, lipids on the surface may act as an insulating intermediate layer, impairing heat conduction and local heating-up of the polymer. This view is supported by the diverging friction curves of SMC and SM10, as well as by comparable final COFs (≈ 0.6) for SM10 and SM100 (Fig. 6).

Second, Ludema and Tabor explained the increase in friction with sliding speed by an increase in shear strength, associated with the viscoelastic bulk material properties of rubbers and polymers and their effects on the shear strength and contact area [47]. With increasing sliding velocity, the force to shear the interface and to break adhesive bonds increases, so that friction rises ("adhesion-shearing theory" [48]). The low COFs observed for both lipid-coated skin models indicate an effective reduction of shear strength in comparison to SMC (Fig. 6). In addition, the relatively constant COF for SM100 might result from a strong reduction of interfacial shear strength provided by the substantial amount of lipids.

Third, polymer friction is associated with shear-induced excitation and delayed relaxation (hysteresis) of polymer chains, due to which energy is dissipated. Greater sliding velocities would increase the hysteresis component of friction and contribute to an increase in friction with sliding speed. This effect has been reported for the rolling friction of a steel ball on polymers [48], and is applicable to lubricated sliding due to the equivalence of rolling and lubricated sliding [42]. Hysteresis is primarily determined by the mechanical bulk properties of the Lorica substrate and can be assumed to be independent of the presence of lipid films on the surface.

Therefore, we believe that the observed increases in the COF as a function of sliding speed are mainly caused by varying interfacial shear strength and adhesion in combination with thermal effects, the latter being unimportant for SM100 and most pronounced for SMC.

3.4 Friction Experiments: Influence of Normal Load

The influence of normal load on the COF of a steel ball against selected skin model surfaces is illustrated in Fig. 7.

The COF of the steel ball against the SMC and SM10 was characterised by an increase of about 0.1 and 0.15, respectively, when the normal load was varied between 1 and 20 N. This behaviour can be explained by an increase in contact area, which results in higher energy dissipation per unit sliding area and a greater adhesion component of friction. However, adhesion effects are normally associated
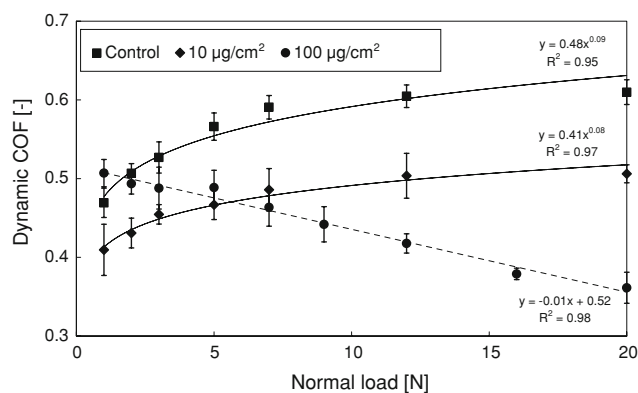
Fig. 7 Influence of normal load on the COF of a steel ball against different skin model surfaces. Data show the mean ± 1SD ($n = 4$) after 100 friction cycles with a mean sliding speed of 8.4 mm/s

with COFs decreasing with normal load [42, 49, 50]. For human skin in the natural/dry condition, adhesion is considered to be the main cause of friction with minor contributions of deformation in the form of hysteresis [20, 50]. We have recently reported constant COFs of about 0.40 [15] for dry skin (index finger) rubbed against a wool fabric. The relatively constant in vivo skin-COFs in a similar normal load range (up to 15 N) indicate that both adhesion and deformation (hysteresis) contribute to skin-friction. Deformation was found to be important for skin-friction not only at increasing sliding speeds [24], but also at high contact pressures [22–24, 51].

Hysteresis losses [43] and ploughing [24] can increase the deformation component of friction (Eq. 1). One can reasonably assume that the deformation term increases with normal load due to ploughing of the steel ball through the soft, compliant polymer substrate, thereby producing grooves in the sliding contact interface if the shear and/or yield strength of the polymer is exceeded, i.e., plastic deformation occurs (Fig. 9). Tang et al. [24] reported a plough model for a sphere sliding on human skin to quantify the deformation component involved in the friction. They derived the following expression:

$$\mu_{ploughing} = \frac{4a}{3\pi r} \qquad (2)$$

with r being the radius of the sphere and a the radius of the contact zone, determined on the basis of force–deformation curves of the solvent-treated Lorica substrate when indented by the steel ball [31]. Using the projected contact area, i. e., spherical segment at indentation depth of the sphere, the contact radius a was determined, and the ploughing component of friction was calculated as a function of the indentation depth and normal load, respectively, according to Eq. 2.

When plotting the relationship between normal load and the ploughing component of friction (Fig. 8), the curve
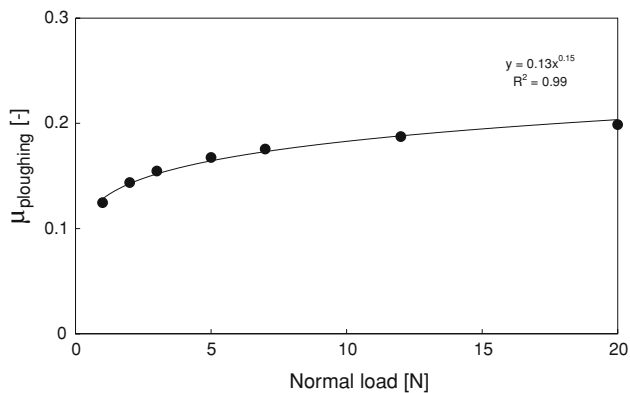
Fig. 8 Influence of normal load on the ploughing component of friction, according to the model proposed by Tang et al. [24]

shape and the fit obtained for the curve are similar to that found for SMC and SM10 (Fig. 7). This indicates that the increase in friction with normal load can be attributed to greater ploughing. In particular, the power-law exponent of 0.15 obtained from the curve fit (Fig. 8) is close to that for SMC (0.09) and SM10 (0.08) and supports this hypothesis. In recent articles, power-law fits have been used to investigate the predominant friction mechanism involved in skin-tribological experiments [20, 22]. In general, friction mechanisms such as adhesion, deformation and hydrodynamic lubrication should be indicated by distinctive exponents of $-1/3$, $+1/3$ and -1, respectively [22].

The most striking result was observed in friction measurements against SM100. The COF of the steel ball in contact with SM100 linearly decreased with normal load from 0.51 at 1 N to 0.35 at 20 N.

During the sliding, the Lorica substrate becomes stretched behind the moving steel ball, whereas a prow wave and piling-up of lipids occur in front of the steel sphere (exemplarily shown in the inserts of Fig. 10), in particular at higher normal loads if the thick sebum coating is scratched from the substrate and deteriorated. This disruption of lipids imbalances and decreases attractive forces acting on the steel ball, and leads to lower COFs.

In addition, with increasing load and due to flattening of the compliant surface asperities, the lipid film thickness in the contact zone may approximate or equal the resulting micro-roughness of Lorica so that a transition from boundary to mixed lubrication can take place. In the mixed lubrication regime, the normal load is partly supported by hydrodynamic pressures generated within the lipid lubricant retained in the spaces between the contacting asperities [52, 53]. This hypothesis includes the assumption that a viscoplastic deformation of the skin model (e.g. due to ploughing, Fig. 9a1) is taking place, enlarging the load-bearing area whereby hydrodynamic forces become capable of supporting the load.

We believe that the increase in the COF with normal load for SMC and the low lipid content surface SM10 (Fig. 7) is due to ploughing effects. Ploughing is, however, unexpected and relatively unlikely for human skin because the mechanical properties of the soft subsurface tissue (i.e., collagen/elastin fibre–water network of the dermis and subcutaneous fat) provide an efficient buffer for high mechanical loads. In a very recent study of our group, we found no evidence for plastic deformation of the skin (index finger and hand) after friction contacts at normal loads up to 50 N [22]. The decrease in the COF observed for SM100 is probably caused by considerable reduction of adhesive forces (due to disruption and deterioration of adhering lipid clusters or even of well-formed lipid menisci), in combination with a transition to mixed lubrication (characterised by flattening of the surface asperities and compacting of the lipids, thereby filling in surface interspaces, Fig. 9b1).

3.5 Friction Experiments: Influence of Slider Material

The influence of varying physico-chemical properties of materials in friction contacts against the skin-model surfaces was studied for two hydrophilic, high-SFE (glass, steel), as well as two hydrophobic, low-SFE (PP, PTFE) spheres (Table 4).

When plotting the COFs of the steel/glass ball against lipid concentration, U-shaped friction graphs were obtained (Fig. 10), being characterised by three prominent points. The highest COF was measured against the SMC (Fig. 10, insert 1). Without lipids, the ISS and adhesion of the steel/glass ball to the SMC are high. The friction of both spheres reaches its minimum at a lipid concentration of ≈ 25 μg/cm^2 (Fig. 10, insert 2), where the ISS is strongly reduced. In regime A (Fig. 10), lipids probably decrease interfacial shear strength and suppress adhesion, leading to lower COFs. As lipid concentrations exceed 25 μg/cm^2 (regime B), the relative importance of RCA and adhesion caused/enhanced by lipids sticking to the spheres (Fig. 10, insert 3) greatly increases and may become more important than the low shear strength of the lipid layer, leading to a gradual rise in the COF. Such a behaviour was also found for human skin with increasing amounts of surface lipids by Gupta et al. [16], who reported on a tendency to higher COFs between steel and the volar forearm, when sebum levels varied between 5 and 18 μg/cm^2.

Steel and glass behaved comparably in general and displayed the highest COFs (0.45–0.7)—greater than those of both polymers. This finding is in accordance with Caravia et al. [52], who reported no significant differences between the COFs of a polyurethane sheet against smooth steel and glass spheres.

Elkhyat et al. [18] furthermore reported that hydrophobic spheres such as PTFE (Ø 10 mm, PTFE: COF = 0.18)
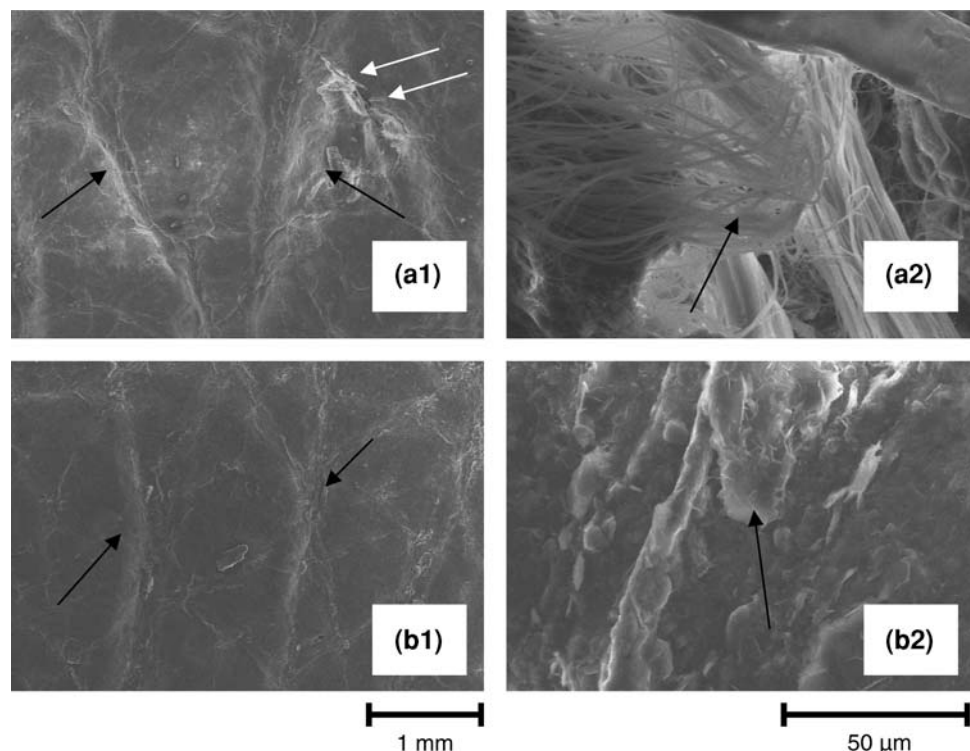
Fig. 9 SEM micrographs of two different skin model surfaces after friction experiments (100 cycles, normal load: 20 N) against a steel ball: **a** Compared to the as-fabricated surface (Fig. 3a), the solvent-treated control surface shows considerable deformation/bulges as well as deterioration in form of a crack/fissure (**a1**, white arrows). The bright fringes (black arrows, **a1**) are no charging artefacts, but rather indicate irregular surface morphology (elevations and steep flanks caused by ploughing) leading to higher signal intensity by emitted secondary electrons. Polyamide-microfibres of the bulk substrate

Lorica are clearly visible in the crack zone (**a2**). The deformation indicates that the shear strength of the underlying PA-fleece is exceeded. **b** Compared to the as-prepared film surface (Fig. 3b), the lipids of the 100 µg/cm^2 skin model surface appear flattened and compressed (**b2**), and seem to partially bridge and fill the interstices of the surface microstructure. Only slight irreversible deformations caused by ploughing actions are visible (**b1**). The friction trace can be observed in the form of a concave impression of the steel ball (arrow, **b2**)
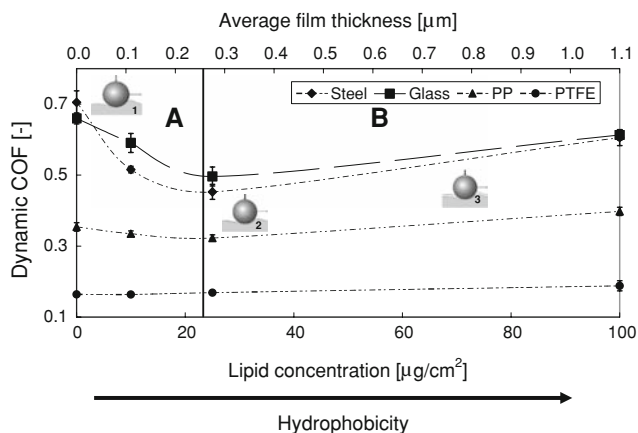
Fig. 10 Influence of slider materials on the dynamic COF against different lipid-coated skin model surfaces after 100 cycles. Friction tests ($n = 5$) were carried out with a normal load of 2 N and a mean sliding speed of 50 mm/s. For illustration, the lipid bridges around the sphere have been exaggerated

Table 4 Surface-chemical properties of the slider materials. Static water contact angles ($n = 5$) were directly measured after gentle cleaning with 70% ethanol for ≈ 5 s. Symbols see Table 3

Slider material	Water CA (°)	γ_s (mN/m)	γ_S^D (mN/m)	γ_S^P (mN/m)
Glass	39.0 ± 2.9	54.7	22.9	31.9
Steel	67.6 ± 2.8	42.9	29.9	13.0
PP	94.0 ± 2.5	28.9	27.2	1.7
PTFE	98.0 ± 3.1	26.1	25.0	1.1

sliding against sebum-poor volar forearm skin (≤ 10 µg/cm^2 [1, 32]) showed much lower friction than hydrophilic spheres (steel: COF = 0.42, glass: COF = 0.74), which is in line with the results of this study measured on the 10 µg/cm^2 skin model surface (Fig. 10). For higher lipid contents (100 µg/cm^2), however, the curve in Fig. 10 probably is not representative of in vivo skin-friction behaviour because the physico-chemical properties of the skin model

surfaces (SFE, hydrophobicity) are different from those reported for more hydrated, high-lipid skin regions such as the forehead (see Sect. 3.1). Forehead skin is characterised by a higher hydrophilicity and SFE [26], as well as higher friction. For example, COFs of 0.34 and 0.26 were measured on the forehead and volar forearm, respectively [17].

For both polymers, the friction was found to be relatively constant and independent of the lipid amount applied to the skin-model substrate. The reduced COF for PP (0.40) and PTFE (0.16) can be explained by the lower interfacial shear strength coming from lower inter-molecular cohesion energies [48, 54, 55].

Green et al. reported that hydrophobic, low-SFE surfaces in contact showed the lowest adhesion and friction [56]. On this basis, the strong decrease in the friction of steel and glass (Fig. 10, regime A) can be explained by surface-chemical interactions driven by differences in the SFE. Glass and steel probably tend to strongly interact with the low SFE skin model lipid surfaces (Table 3) in order to reduce or minimise their high SFE (43–55 mN/m). In this process, lipids may be "elicited and attracted" to cover their surfaces as mono-layers, thereby reducing and adapting the SFE towards that of the skin-model surface, which would explain the strong decrease in the friction. It has been concluded that the COF of a steel ball increases, as the SFE of its polymer counter-face (PP) increases [46], which would support the above hypothesis.

The influence of lipid concentration on friction was much less pronounced in the case of PP and PTFE. Due to their low SFE and high hydrophobicity (Table 4), there is probably little physico-chemical interaction between the solid polymer sliders and the amphiphilic lipids, leading to relatively constant interfacial shear strength, adhesion and COFs over the range of investigated lipid concentrations. Material transfer of PP or PTFE onto the underlying skin-model substrate could be an additional factor for the constant friction traces. PTFE transfer was confirmed by X-ray photoelectron spectroscopy (XPS 5600 LS, Physical Electronics, Ismaning, Germany).

Although cleaning with low-surface-tension agents (70% ethanol, 23.8 mN/m) cannot be ignored and affects the physico-chemical surface properties, the results for the different materials (Table 4) demonstrated clear differences allowing the categorisation into hydrophilic, high-SFE (glass, steel) and hydrophobic, low-SFE (PP, PTFE) sliders.

3.6 Study Limitations

To the authors' knowledge, there is no literature available on the formation, assembly and orientation/arrangement of sebum lipids on the skin surface. Therefore, a simple spray method was used to prepare sebum films of relevance to the in vivo skin situation, with the aim of demonstrating the feasibility of lipid-coated skin model surfaces. The main focus was placed on the bio-mimetics of the lipid surface chemistry rather than on the investigation of lipid structure, conformation and molecular orientation.

The manual spraying process is labour intensive and a substantial part of the lipid solution can be lost into the air. Therefore, imperfections and film inhomogeneities cannot be completely ruled out. Homogeneous lipid coatings and an improved reproducibility could be obtained by automated vapourisers [10]. The theoretical calculation of the nominal film thickness assumes a homogeneous thickness distribution of the lipids, which could be analysed and checked by surface mapping using atomic force microscopy.

Contact angle measurements on the rough skin model surfaces provide relative rather than absolute values of the SFE, allowing cross-comparisons of the different lipid coatings on the same substrate if wetting phenomena (e.g. hemi-wicking and pinning [57] can be excluded or neglected. Such effects played a negligible role in our experiments, so that differences in the SFE can plausibly explain the friction results shown in Sect. 3.5.

4 Summary and Outlook

An artificial sebum formulation was applied in physiologically relevant concentrations ($\leq$100 μg/cm^2) to an existing mechanical skin-model substrate in order to simulate the lipidic surface chemistry of human skin. The lipid-coated skin models demonstrated lubrication effects over a wide range of sliding velocities and normal loads. On the skin models, COFs of spherical sliders increased with sliding velocity, which can be attributed to greater adhesion due to increase in ISS. For lipid-coated skin models with lipid concentrations of $\leq$10 μg/cm^2, COFs increased with normal load probably due to a greater ploughing component of friction. The decreasing trend in the COF found for the 100 μg/cm^2 lipid film surface indicates considerable reduction of adhesive forces, in combination with a transition to mixed lubrication.

In friction experiments with lipid films of increasing thickness, U-shaped friction curves were obtained for the hydrophilic, high-SFE materials (steel, glass), with the lowest COF ($\approx$0.5) against skin-model surfaces with 25 μg/cm^2 lipids. For both hydrophobic, low-SFE polymers tested, the COF was considerably lower (0.4 for PP, 0.16 for PTFE) and relatively independent of the lipid amount, indicating that both mechanical and surface-chemical properties of the sliders strongly influence the friction behaviour on the skin model surfaces.

In future research, a detailed study on the correlation between COFs determined against the skin models in

comparison with those measured on human skin is necessary to validate the present skin models.

The orientation and organisation of the sebum lipids on the skin model remain to be explored in detail. Skin-model surfaces with ≤ 25 µg/cm^2 lipids seem to realistically simulate the physico-chemical properties of dry, sebum-poor skin regions. The development of a refined hydro-lipid skin model might also permit water-content variation and adjustment to physiological skin conditions. In particular, sebum-coated skin models with a porous surface and a compliant subsurface might be an advanced and more versatile tool for objectively studying friction and adhesion, as well as wetting behaviour and dynamic penetration mechanisms of liquids and emulsions on simulated dry and wet skin surface conditions, not only for tribologists but also for cosmetic chemists.

References

1. Agache, P., Humbert, P.: Measuring the Skin—Non-Invasive Investigations, Physiology, Normal Constants. Springer-Verlag, Berlin (2004)
2. Elias, P.M.: Epidermal lipids, barrier function, and desquamation. J. Invest. Dermatol. **80**, 44S–49S (1983). doi:10.1111/1523-1747.ep12537108
3. Michniak, B.B., Wertz, P.W.: Water-lipid interactions. In: Fluhr, J.W., Elsner, P., Berardesca, E., Maibach, H.I. (eds.) Bioengineering of the Skin: Water and the Stratum Corneum, pp. 3–14. CRC Press, Boca Raton (2005)
4. Bouwstra, J.A., Gooris, G.S., Cheng, K., Weerheim, A., Bras, W., Ponec, M.: Phase behavior of isolated skin lipids. J. Lipid Res. **37**, 999–1011 (1996)
5. Bouwstra, J.A., Gooris, G.S., Dubbelaar, F.E., Ponec, M.: Phase behavior of lipid mixtures based on human ceramides: coexistence of crystalline and liquid phases. J. Lipid Res. **42**, 1759–1770 (2001)
6. de Jager, M.W., Gooris, G.S., Ponec, M., Bouwstra, J.A.: Lipid mixtures prepared with well-defined synthetic ceramides closely mimic the unique stratum corneum lipid phase behavior. J. Lipid Res. **46**, 2649–2656 (2005). doi:10.1194/jlr.M500221-JLR200
7. Laugel, C., Yagoubi, N., Baillet, A.: ATR-FTIR spectroscopy: a chemometric approach for studying the lipid organisation of the stratum corneum. Chem. Phys. Lipids **135**, 55–68 (2005). doi:10.1016/j.chemphyslip.2005.02.001
8. Moore, D.J., Snyder, R.G., Rerek, M.E., Mendelsohn, R.: Kinetics of membrane raft formation: fatty acid domains in stratum corneum lipid models. J. Phys. Chem. B **110**, 2378–2386 (2006). doi:10.1021/jp054875h
9. de Jager, M., Groenink, W., van der Spek, J., Janmaat, C., Gooris, G., Ponec, M., Bouwstra, J.: Preparation and characterization of a stratum corneum substitute for in vitro percutaneous penetration studies. Biochim. Biophys. Acta Biomembr. **1758**, 636–644 (2006). doi:10.1016/j.bbamem.2006.04.001
10. Groen, D., Gooris, G.S., Ponec, M., Bouwstra, J.A.: Two new methods for preparing a unique stratum corneum substitute. Biochim. Biophys. Acta Biomembr. **1778**, 2421–2429 (2008). doi:10.1016/j.bbamem.2008.06.015
11. Charkoudian, J.C.: A model skin surface for testing adhesion to skin. J. Soc. Cosmet. Chem. **39**, 225–234 (1988)
12. Bhuyan, S., Sundararajan, S., Yao, L., Hammond, E.G., Wang, T.: Boundary lubrication properties of lipid-based compounds evaluated using microtribological methods. Tribol. Lett. **22**, 167–172 (2006). doi:10.1007/s11249-006-9076-x
13. Elleuch, K., Elleuch, R., Zahouani, H.: Comparison of elastic and tactile behavior of human skin and elastomeric materials through tribological tests. Polym. Eng. Sci. **46**, 1715–1720 (2006). doi:10.1002/pen.20637
14. Ramkumar, S.S., Wood, D.J., Fox, K., Harlock, S.C.: Developing a polymeric human finger sensor to study the frictional properties of textiles. Part I: artificial finger development. Text. Res. J. **73**, 469–473 (2003). doi:10.1177/004051750307300601
15. Derler, S., Schrade, U., Gerhardt, L.-C.: Tribology of human skin and mechanical skin equivalents in contact with textiles. Wear **263**, 1112–1116 (2007). doi:10.1016/j.wear.2006.11.031
16. Gupta, A.B., Haldar, B., Bhattacharya, M.: A simple device for measuring skin friction. Int. J. Dermatol. **40**, 116–121 (1995)
17. Cua, A.B., Wilhelm, K.P., Maibach, H.I.: Skin surface lipid and skin friction: relation to age, sex and anatomical region. Skin Pharmacol. **8**, 246–251 (1995)
18. Elkhyat, A., Courderot-Masuyer, C., Gharbi, T., Humbert, P.: Influence of the hydrophobic and hydrophilic characteristics of sliding and slider surfaces on friction coefficient: in vivo human skin friction comparison. Skin Res. Technol. **10**, 215–221 (2004). doi:10.1111/j.1600-0846.2004.00085.x
19. Sivamani, R.K., Goodman, J., Gitis, N.V., Maibach, H.I.: Coefficient of friction: tribological studies in man—an overview. Skin Res. Technol. **9**, 227–234 (2003). doi:10.1034/j.1600-0846.2003.02366.x
20. Adams, M.J., Briscoe, B.J., Johnson, S.A.: Friction and lubrication of human skin. Tribol. Lett. **26**, 239–253 (2007). doi:10.1007/s11249-007-9206-0
21. Gerhardt, L.-C., Strässle, V., Lenz, A., Spencer, N.D., Derler, S.: Influence of epidermal hydration on the friction of human skin against textiles. J. R. Soc. Interface **5**, 1317–1328 (2008). doi:10.1098/rsif.2008.0034
22. Derler, S., Gerhardt, L.-C., Lenz, A., Bertaux, E., Hadad, M.: Friction of human skin against smooth and rough glass as a function of the normal load. Tribol. Int. (in press). doi:10.1016/j.triboint.2008.11.009
23. Ramalho, A., Silva, C.L., Pais, A.A.C.C., Sousa, J.J.S.: In vivo friction study of human skin: influence of moisturizers on different anatomical sites. Wear **263**, 1044–1049 (2007). doi:10.1016/j.wear.2006.11.051
24. Tang, W., Ge, S.-R., Zhu, H., Cao, X.-C., Li, N.: The influence of normal load and sliding speed on frictional properties of skin. J. Bionic Eng. **5**, 33–38 (2008). doi:10.1016/S1672-6529(08)60004-9
25. Elkhyat, A., Mavon, A., Leduc, M., Agache, P., Humbert, P.: Skin critical surface tension—a way to assess the skin wettability quantitatively. Skin Res. Technol. **2**, 91–96 (1996). doi:10.1111/j.1600-0846.1996.tb00066.x
26. Mavon, A., Zahouani, H., Redoules, D., Agache, P., Gall, Y., Humbert, P.: Sebum and stratum corneum lipids increase human skin surface free energy as determined from contact angle measurements: A study on two anatomical sites. Colloids Surf. B Biointerfaces **8**, 147–155 (1997). doi:10.1016/S0927-7765(96)01317-3

27. Stefaniak, A.B., Harvey, C.J.: Dissolution of materials in artificial skin surface film liquids. Toxicol. In Vitro **20**, 1265–1283 (2006). doi:10.1016/j.tiv.2006.05.011

28. Stefaniak, A.B., Harvey, C.J., Wertz, P.W.: Artificial skin surface film liquids. Part 1: formulation and stability of sebum under conditions of storage and use. Clin. Exp. Dermatol. (submitted)

29. Lagarde, J.M., Rouvrais, C., Black, D.: Topography and anisotropy of the skin surface with ageing. Skin Res. Technol. **11**, 110–119 (2005). doi:10.1111/j.1600-0846.2005.00096.x

30. Li, L., Mac-Mary, S., Marsaut, D., Sainthillier, J.M., Nouveau, S., Gharbi, T., de Lacharriere, O., Humbert, P.: Age-related changes in skin topography and microcirculation. Arch. Dermatol. Res. **297**, 412–416 (2006). doi:10.1007/s00403-005-0628-y

31. Gerhardt, L.-C.: Tribology of human skin in contact with medical textiles for decubitus prevention. Ph.D. thesis, ETH Zurich, Zurich (2008)

32. Sheu, H.M., Chao, S.C., Wong, T.W., Yu-Yun Lee, J., Tsai, J.C.: Human skin surface lipid film: an ultrastructural study and interaction with corneocytes and intercellular lipid lamellae of the stratum corneum. Br. J. Dermatol. **140**, 385–391 (1999). doi:10.1046/j.1365-2133.1999.02697.x

33. Mashaghi, A., Swann, M., Popplewell, J., Textor, M., Reimhult, E.: Optical anisotropy of supported lipid structures probed by waveguide spectroscopy and its application to study of supported lipid bilayer formation kinetics. Anal. Chem. **80**, 3666–3676 (2008). doi:10.1021/ac800988v

34. Kaelble, D.H.: Dispersion-polar surface tension properties of organic solids. J. Adhes. **2**, 66–81 (1970). doi:10.1080/00218467 08544582

35. Owens, D.K., Wendt, R.C.: Estimation of surface free energy of polymers. J. Appl. Polym. Sci. **13**, 1741–1747 (1969). doi:10.1002/app.1969.070130815

36. Rabel, W.: Flüssigkeitsgrenzflächen in Theorie und Anwendungstechnik. Phys. Blätt. **33**, 151–161 (1977)

37. Walther, F., Davydovskaya, P., Zürcher, S., Kaiser, M., Herberg, H., Gigler, A.M., Stark, R.W.: Stability of the hydrophilic behavior of oxygen plasma activated SU-8. J. Micromech. Microeng. **17**, 524–531 (2007). doi:10.1088/0960-1317/17/3/015

38. Gerhardt, L.-C., Mattle, N., Schrade, G.U., Spencer, N.D., Derler, S.: Study of skin-fabric interactions of relevance to decubitus: friction and contact-pressure measurements. Skin Res. Technol. **14**, 77–88 (2008). doi:10.1111/j.1600-0846.2007.00264.x

39. Albertorio, F., Chapa, V.A., Chen, X., Diaz, A.J., Cremer, P.S.: The α, α-(1 → 1) linkage of trehalose is key to anhydrobiotic preservation. J. Am. Chem. Soc. **129**, 10567–10574 (2007). doi:10.1021/ja0731266

40. Burton, J.L.: The physical properties of sebum in acne vulgaris. Clin. Sci. **39**, 757–767 (1970)

41. Elkhyat, A., Agache, P., Zahouani, H., Humbert, P.: A new method to measure in vivo human skin hydrophobia. Int. J. Cosmet. Sci. **23**, 347–352 (2001). doi:10.1046/j.0412-5463.2001.00108.x

42. Moore, D.F.: The Friction and Lubrication of Elastomers. Pergamon Press, Oxford, UK (1972)

43. Greenwood, J.A., Tabor, D.: The friction of hard sliders on lubricated rubber: the importance of deformation losses. Proc.

44. Mate, C.M.: Nanotribology of lubricated and unlubricated carbon overcoats on magnetic disks studied by friction force microscopy. Surf. Coat. Technol. **63**, 373–379 (1993). doi:10.1016/0257-8972(93)90270-X

45. Birley, A.W., Haworth, B., Batchelor, J.: Hardness, friction, surface abrasion and wear. In: Birley, A., Haworth, B., Batchelor, J. (eds.) Physics of Plastics: Processing, Properties and Materials Engineering, pp. 320–326. Hanser Verlag, Munich, Germany (1992)

46. Hornbogen, E., Schäfer, K.: Friction and wear of thermoplastic polymers. In: Rigney, D.A. (ed.) Fundamentals of Friction and Wear of Materials, pp. 409–438. American Society for Metals, Metals Park, Ohio (1981)

47. Ludema, K.C., Tabor, D.: The friction and visco-elastic properties of polymeric solids. Wear **9**, 329–348 (1966). doi:10.1016/0043-1648(66)90018-4

48. Yamaguchi, Y.: Friction. In: Yamaguchi, Y. (ed.), Tribology of Plastic Materials: Their Characteristics and Applications to Sliding Components, pp. 1–91. Elsevier Science Publishers B.V., Amsterdam, The Netherlands (1990)

49. Koudine, A.A., Barquins, M., Anthoine, P.H., Aubert, L., Lévêque, J.-L.: Frictional properties of skin: proposal of a new approach. Int. J. Cosmet. Sci. **22**, 11–20 (2000). doi:10.1046/j.1467-2494.2000.00006.x

50. Wolfram, L.J.: Friction of skin. J. Soc. Cosmet. Chem. **34**, 465–476 (1983)

51. Derler, S., Huber, R., Feuz, H.-P., Hadad, M.: Influence of surface microstructure on the sliding friction of plantar skin against hard substrates. Wear (accepted)

52. Caravia, L., Dowson, D., Fisher, J., Corkhill, P.H., Tighe, B.J.: Friction and mixed lubrication in soft layer contacts. In: Dowson, D., Taylor, C.M., Childs, T.H.C., Godet, M., Dalmaz, G. (eds.) Thin Films in Tribology, pp. 529–534. Elsevier Science Publishers B.V., Amsterdam, The Netherlands (1993)

53. Dowson, D.: Tribology and the skin surface. In: Wilhelm, K.-P., Elsner, P., Berardesca, E., Maibach, H.I. (eds.) Bioengineering of the Skin: Skin Surface Imaging and Analysis, 1st edn, pp. 159–180. CRC Press, Boca Raton (1997)

54. Callister, J.W.D.: Materials science and engineering: an introduction, 6th edn. John Wiley & Sons, Inc., Hoboken, NJ, USA (2003)

55. Myshkin, N.K., Petrokovets, M.I., Kovalev, A. V.: Tribology of polymers: adhesion, friction, wear, and mass-transfer. Tribol. Int. **38**, 910–921 (2005). doi:10.1016/j.triboint.2005.07.016

56. Green, J.-B.D., McDermott, M.T., Porter, M.D., Siperko, L.M.: Nanometer-scale mapping of chemically distinct domains at well-defined organic interfaces using frictional force microscopy. J. Phys. Chem. **99**, 10960–10965 (1995). doi:10.1021/j100027a041

57. Spori, D.M., Drobek, T., Zürcher, S., Ochsner, M., Sprecher, C., Mühlebach, A., Spencer, N.D.: Beyond the lotus effect: roughness influences on wetting over a wide surface-energy range. Langmuir **24**, 5411–5417 (2008). doi:10.1021/la800215r

Phys. Soc. Lond. **71**, 989–1001 (1958). doi:10.1088/0370-1328/71/6/312